Neotropical Ichthyology

Original article

https://doi.org/10.1590/1982-0224-2024-0025

urn:lsid:zoobank.org:pub:00141B86-614C-4865-9079-EE651CCD3B99

A new species of the tridentine *Rhinotridens* from the Amazon basin (Siluriformes: Trichomycteridae)

Correspondence:
Mário de Pinna
pinna@ib.usp.br

Mário de Pinna, Vinícius Reis, Murilo N. L. Pastana and Aléssio Datovo

A new species of the recently discovered miniature tridentine catfish, *Rhinotridens*, is described from the Amazon basin in Brazil, Colombia, and Peru. It differs from *Rhinotridens chromocaudatus*, type-species of the genus, in having the caudal fin mostly hyaline, a rictal barbel vestigial or externally absent, a longer anal fin with 22–29 segmented rays, and numerous other features from the skeleton. An osteological account of the new species is provided based on cleared and stained specimens, and traits of its external morphology are revealed through scanning electron microscopy (SEM), which for the first time reveal details of the lip structure of tridentines. The seven morphological characters previously listed as synapomorphies for *Rhinotridens* are confirmed in the species described herein, corroborating its generic allocation. An additional characteristic from the morphology of the lateral process of the autopalatine is proposed as a novel synapomorphy for the genus.

Keywords: Candiru, Catfish, Miniature, Systematics, Taxonomy.

Submitted March 15, 2024
Accepted May 24, 2024
by Carlos DoNascimiento
Epub July 22, 2024

Online version ISSN 1982-0224
Print version ISSN 1679-6225

Neotrop. Ichthyol.
vol. 22, no. 2, Maringá 2024

Museu de Zoologia da Universidade de São Paulo, Caixa Postal 42494, 04218-970 São Paulo, SP, Brazil. (MP) pinna@ib.usp.br (corresponding author), (VR) carvalhvinicius@gmail.com, (MNLP) mpastana@usp.br, (AD) adatovo@usp.br.

Uma nova espécie do recentemente descoberto tridentíneo miniatura, *Rhinotridens*, é descrita da bacia Amazônica no Brasil, Colômbia e Peru. A nova forma difere de *Rhinotridens chromocaudatus*, espécie-tipo do gênero, pela nadadeira caudal hialina, o barbilhão rictal vestigial ou externamente ausente, a nadadeira anal longa, com 22–29 raios segmentados, além de várias outras características do esqueleto. Uma descrição osteológica da nova espécie é fornecida com base em exemplares diafanizados e corados, e características de morfologia externa são revelados através de microscopia eletrônica de varredura (MEV), que pela primeira vez mostram detalhes da estrutura labial de Tridentinae. Os sete caracteres morfológicos previamente listados como sinapomorfias de *Rhinotridens* são confirmados na espécie aqui descrita, corroborando sua alocação genérica. Uma característica adicional da morfologia do processo lateral do autopalatino é proposta como uma nova sinapomorfia do gênero.

Palavras-chave: Bagre, Candiru, Miniatura, Sistemática, Taxonomia.

INTRODUCTION

The genus *Rhinotridens* Datovo, Ochoa, Vita, Presti, Ohara & de Pinna, 2023 was recently described to include a single new species from the rio Purus system in the Amazon basin. The new genus was proposed as sister group to *Tridens* Eigenmann & Eigenmann, 1889 plus *Tridensimilis* Schultz, 1944 on the basis of direct morphological data. Preliminary evidence for a second species in the genus was reported in the original publication, but held off awaiting more detailed studies. Herein we present results of additional research done on that potential taxon, confirming it as a new species and the second one in *Rhinotridens*.

A total of five tridentine genera are currently recognized, *Miuroglanis* Eigenmann & Eigenmann, 1889, *Tridens*, *Tridentopsis* Myers, 1925, *Tridensimilis*, and *Rhinotridens*, comprising a total of ten species, all of which are miniatures (Weitzman, Vari, 1988). The composition of Tridentinae has been stable since its establishment in Eigenmann (1918) and its monophyly has been repeatedly corroborated on both morphological and partly on molecular evidence (Baskin, 1973; de Pinna, 1998; DoNascimiento, 2013; Ochoa *et al*., 2017, 2020; Reis, 2022; Reis *et al*., *in press*). The genus *Potamoglanis* Henschel, Mattos, Katz & Costa, 2017 (formerly "*Trichomycterus*" *hasemani* group) was considered by de Pinna (1989) as closely related to the traditional Tridentinae and included in the latter subfamily by Henschel *et al*. (2017) on the basis of molecular and morphological data. That hypothesis has been refuted in subsequent studies which included the genus as sister-group of the TSV-clade (Wosiacki, 2002; DoNascimiento, 2015; Reis, 2022; Reis *et al*., *in press*), or sister-group of Glanapteryginae (Reis, 2022; Reis *et al*., *in press*), or sister-group of Sarcoglanis simplex (Ochoa *et al*., 2017); or sister-group of Glanapteryginae plus Sarcoglanidinae (Ochoa *et al*., 2020; Datovo *et al*., 2023). Geographic distribution of Tridentinae includes the Amazon, Orinoco, and Paraguay river basins.

Tridentinae are poorly known in all aspects, including their morphology, both internal and external. They have been considered as the trichomycterid subfamily where the least progress has been made in the past 40 years (de Pinna, 2016) and in

fact may be the least known subfamily of Trichomycteridae overall. In the description of *Rhinotridens chromocaudatus* Datovo, Ochoa, Vita, Presti, Ohara & Pinna, 2023, a survey of the osteology of the species was offered based on CT-Scan data and cleared and stained specimens. For the present contribution, we expanded that coverage to SEM imaging. As with several other small-sized and mostly white trichomycterids, their external morphology is not readily accessible in alcoholic specimens by normal optical methods. In those cases, SEM examination reveals several features hardly – or not at all – visible otherwise, providing previously unsuspected comparative data on the surface of the body (*e.g.*, de Pinna, Kirowsky, 2011; de Pinna, Zuanon, 2013; de Pinna, Dagosta, 2022).

MATERIAL AND METHODS

Morphometric data of body subunits were taken on photographed specimens using a Zeiss Axiocam 506 color digital camera attached to a Zeiss Discovery V20 stereomicroscope, using the "Graphics: line" tool from the Zeiss software Zen 2 pro. Measurements followed de Pinna, Dagosta (2022), except that body depth was taken vertically through pectoral-fin insertion. Principal caudal-fin rays were counted according to Lundberg, Baskin (1969). In other fin counts, unbranched segmented soft rays are represented by simple lower case Roman numerals (*e.g.*, iii), and branched segmented rays by Arabic numerals (*e.g.*, 3). Procurrent rays, when present, are indicated in text. The two posteriormost closely set rays in dorsal and anal fins were counted as separate elements, regardless of their support in the same or separate pterygiophores. Counts were recorded for types and non-type specimens, with absolute frequencies for each value given in parentheses throughout the description, and holotype counts indicated with an asterisk. Numbers of branchiostegals, vertebrae, ribs, number and position of dorsal- and anal-fin support elements, and other osteological features were obtained from paratypes cleared and counterstained according to Taylor, Van Dyke (1985) and Walker, Kimmel (2007) – the latter avoiding the use of acetic acid in their protocol thus enhancing bone visualization in miniature and juvenile specimens. Vertebral counts included all free vertebrae posterior to the Weberian complex, with the compound caudal centrum counted as one. Cephalic pores of the latero-sensory system were stereomicroscopically examined in alcoholic and c&s specimens. Their visibility in SEM photos is partial because of irregular mucus covering in the preparation. Individual pores are mapped and named according to Arratia, Huaquin (1995), specifically with reference to their fig. 9E (of *Tridentopsis* sp.). Anatomical terminology followed Datovo, Bockmann (2010), DoNascimiento (2013), and de Pinna, Dagosta (2022). As in the latter publication, the term odontodophore refers to the opercular and interopercular odontode-bearing complex, including its modified bony base, the periodontodeal integument rim and the odontodes themselves. Odontodophore replaces the English term "patch of odontodes" and multiple variants used in different languages ("Crochet operculaires" in French, "conjunto de odontódios operculares" in Portuguese, "grupo de espinas operculares" in Spanish, "Kiemenstacheln" in German, among many alternatives). The term can be adapted in identical or similar spelling in the vernacular of all those languages (odontodophore in English, odontodophòre in French, odontodophor

in German, odontodóforo in Portuguese and Spanish, etc.). Odontodophore joins a list of odontode-derivative terms long used, such as monodontodia, polyodontodia, odontocomplex, odontodium, etc. (Ørvig, 1977).

Specimens intended for SEM examinations were dehydrated in ethanol series (35%–70%–100%). Once in absolute ethanol, they were freed from superficial sand grains and other consolidated debris adhered to the integument by immersion in an ultrasonic bath for 2 min. Specimens were subsequently critical-point dried (enveloped in a small case of thin paper), gold-coated, and mounted on SEM stubs.

Photographs of cleared and stained preparations were made with a Zeiss Axiocam 506 color digital camera attached to a Zeiss Discovery V20 stereomicroscope. Abbreviations: eth, ethanol preserved specimens; c&s, clear and stained specimens; EPA, Expedição Permanente da Amazônia; sem, SEM specimens; HL, head length; SL, standard length. Institutional abbreviations follow Fricke, Eschmeyer (2023).

RESULTS

Rhinotridens britskii, new species

urn:lsid:zoobank.org:act:D5BECFB8-032B-4A41-B367-A9F5D3992D4E

(Figs. 1–10; Tab. 1)

Holotype. ZUEC 18281, 15.2 mm SL; Brazil, Amazonas State, Atalaia do Norte Municipality, rio Amazonas basin, rio Javari drainage, rio Itacoaí subdrainage (sometimes called Itacoari or Itaquaí), igarapé Boa Vista, upstream from mouth of rio Queixito, 04°26'37"S 70°14'11"W, 15 Nov 2017, F. C. T. Lima, C. R. Moreira, G. N. Salvador & N. Flausino Jr.

Paratypes. Brazil, Amazonas State. MNRJ 55570, 7 eth (14.4–15.8 mm SL), same data as holotype; MZUSP 129867, 8 eth, 2 c&s (13.0–14.8 mm SL), same data as holotype; MZUSP 36302, 11 eth, 4 c&s, 1 sem (12.7–13.8 mm SL), lago Buiuçu, Ati-Paraná, NW of Fonte Boa, *ca*. 01°51'S 65°37'W, 11–12 Oct 1968, EPA; MZUSP 23449, 1 eth (15.7 mm SL), lago Mari-Mari, Ati-Paraná, NW of Fonte Boa, 01°51'58.36"S 66°41'0.65"W, 14 Oct 1968, EPA; ZUEC 15118, 27 eth, 4 c&s (14.7–16.9 mm SL), same data as holotype.

Non-types. MCZ 52186, 4 eth, 1 c&s (disarticulated) (14.1–15.3 mm SL), Colombia, Loreto, Río Loreto-Yacco [= Río Loretoyaco], *ca*. 03°30'S 70°10'W, Nov 1976, C. Navarro; MZUSP 72977, 1 eth (14.8 mm SL), Brazil, Amazonas State, rio Madeira, unnamed igarapé 15 km from Humaitá, *ca*. 07°30'S 63°02'W, 7 Aug 1984, M. Goulding. MZUSP 121256, 1 eth (15.2 mm SL), 14.5 mm SL, Peru, main channel of Río Yanayacu, Río Yana drainage, 03°24'05.2"S 72°04'19.4"W, 21 Oct 2014, M. Toledo-Piza *et al*.

Diagnosis. The new species differs from its single congener, *Rhinotridens chromocaudatus*, by the caudal fin mostly hyaline, with only a few uniformly scattered dark melanophores not forming any particular pattern (Fig. 1; *vs.* chromatophores forming a conspicuous horizontal dark stripe in the middle of the caudal fin); by the rictal barbel externally vestigial or absent (Fig. 2, where it is externally invisible; *vs.* clearly visible externally); by the anal fin with 22–29 segmented rays (*vs.* 17–20); by the interorbital distance larger than eye diameter (Fig. 1; *vs.* equal); by the lateral process of the autopalatine positioned close to the anterior margin of the bone, and with a broad base, straight evenly narrowing to tip (Fig. 3; *vs.* process positioned at middle of the bone, anteriorly curved and of roughly even width); by the lack of lower pharyngeal dentition (Fig. 4; *vs.* two teeth present on ceratobranchial 5); and by the mostly straight orbitosphenoid, parallel to longitudinal axis of skull (Fig. 5; *vs.* curved laterally).

Description. Morphometric data for holotype and paratypes given in Tab. 1. Body elongate, deeper than wide at pectoral-fin insertion and progressively more compressed towards caudal peduncle (Fig. 1). Dorsal profile gently convex from nape to dorsal fin and gently concave or straight from that point to middle of caudal peduncle, then convex again along region of procurrent caudal-fin rays. Ventral profile of body straight to gently convex along cardiac region, then gently convex or straight to anal-fin origin, straight along anal-fin base and convex along posterior half of caudal peduncle. Anal opening immediately anterior to anal-fin origin. Greatest body depth variable, at region ranging from vertical through pelvic-fin base to anus.

FIGURE 1 | *Rhinotridens britskii*, holotype, ZUEC 18281, 15.2 mm SL. Brazil, Amazonas State, Igarapé Boa Vista (rio Purus drainage). **A.** Lateral view; **B.** Dorsal view; **C.** Ventral view.

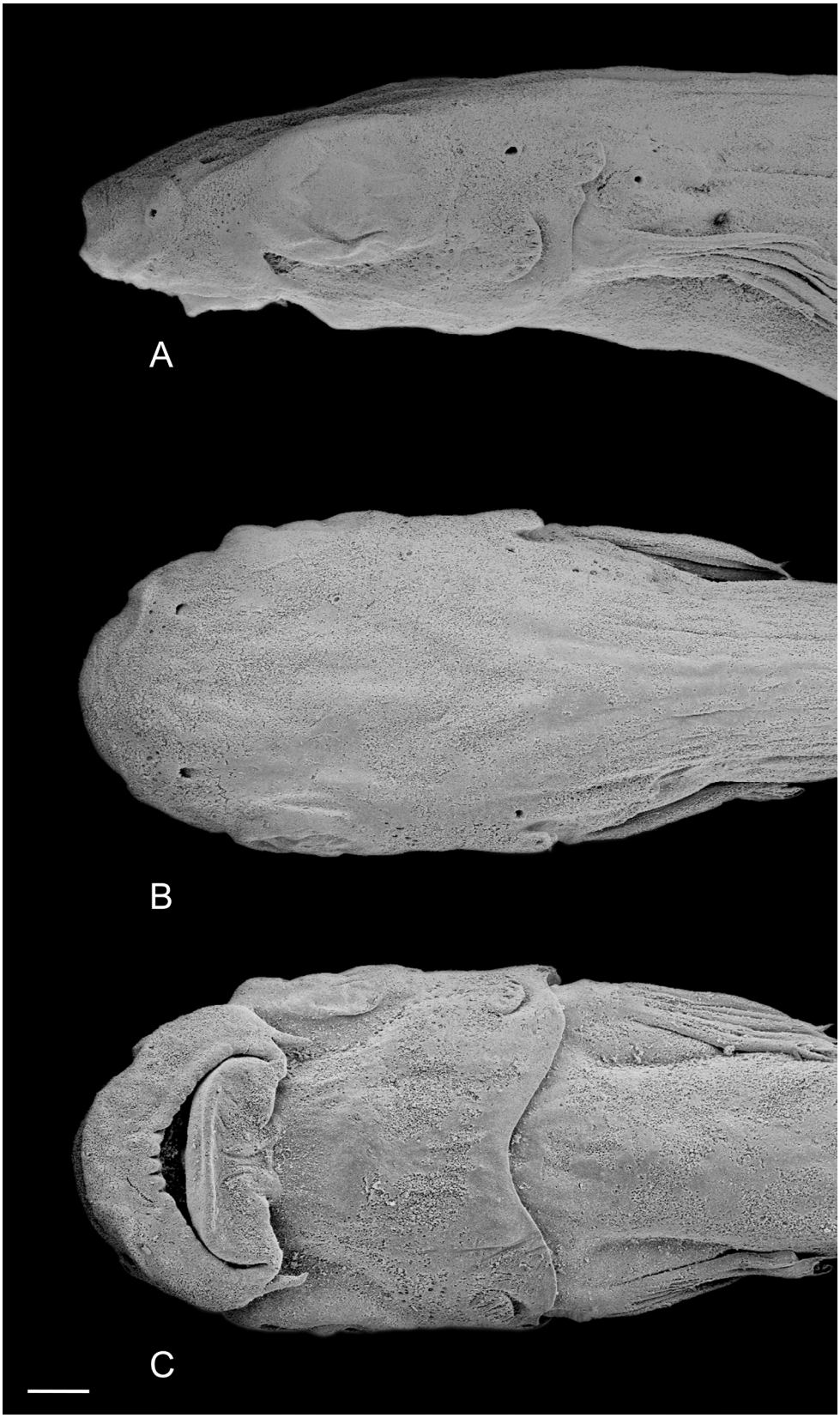

FIGURE 2 | Scanning electron microscopy of the head and anterior part of body of *Rhinotridens britskii*, paratype, MZUSP 36303, 13.4 mm SL. **A.** Lateral view; **B.** Dorsal view; **C.** Ventral view. Scale bar = 0.1 mm.

Head depressed, longer than wide. Snout with semicircular anteromedial protrusion particularly evident in dorsal and ventral views (Figs. 1–2). Anterior nostril small, directed anterolaterally, positioned at margin of head at junction between central protrusion of snout and rest of head, surrounded by short tube of integument (Fig. 2). Anterior nostril more exposed in ventral than in dorsal view. Nasal barbel absent. Posterior nostril round, smaller than anterior one and positioned dorsally on head, slightly closer to anterior nostril than to anterior margin of eye. Posterior nostril lacking tube or rim of integument, extended posteriorly by gently and narrow hydrodynamic ridge. Posterior internarial width smaller than interorbital. Mouth ventral, crescent-shaped, its corners directed posteriorly or even slightly converging towards midline in ventral view. Upper lip thick, its posterior margin gently round, with curvature accentuated centrally and continuous posteriorly with maxillary barbel (Fig. 2C). Lower lip wider than upper one, subdivided into poorly-defined bilateral lobes slanted posteriorly, with anterior margin straight or slightly convex (or with strong central concavity in some specimens, presumably depending on muscle contraction upon fixation). Upper and lower lips continuous via narrow integumentary connection posteriorly. Maxillary barbel reaching anterior half to middle of eyeball. Rictal barbel either vestigial (visible externally as small protrusion in lower lip flap integument), or externally absent (totally embedded in lower lip flap integument, as in specimen in Fig. 2). Internal cores of both barbels well developed, as visible in skeletal preparations stained for cartilage (Fig. 3). Eyes extremely large and round, covered with thin translucent skin not adhered to eyeball's surface. Eyes located laterally on head, at middle of HL and fully visible in both dorsal and ventral views (Fig. 1). Interorbital space larger than eye diameter. Greatest head width at transverse line through posterior margin of eyes. Opercular odontodophore (Fig. 6) small and semicircular at free posterior margin, fully visible in lateral view (in profile in dorsal view) and located immediately dorsal to pectoral-fin base, with 3 exposed conical odontodes. Interopercular odontodophore (Fig. 6) semicircular, twice as large as opercular one,

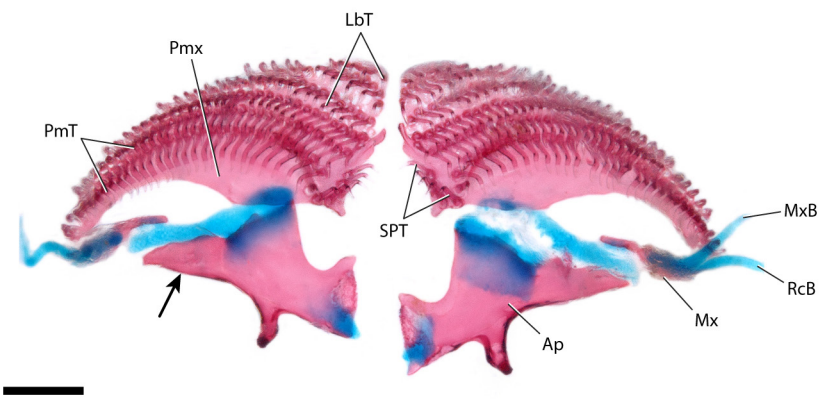

FIGURE 3 | Upper jaw and autopalatine of *Rhinotridens britskii*, paratype, MZUSP 129867, 15.2 mm SL; ventral view. Left anterior autopalatine cartilage damaged. Arrow indicates lateral process of autopalatine. Ap, autopalatine; LbT, labial teeth; Mx, maxilla; MxB, maxillary barbel; PmT, premaxillary teeth; Pmx, premaxilla; RcB, rictal barbel; SPT, symphyseal premaxillary teeth. Scale bar = 0.2 mm.

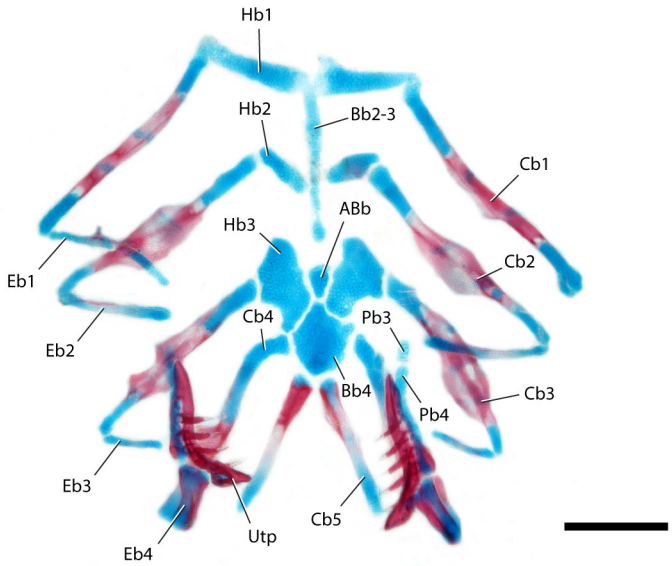

FIGURE 4 | Gill arches of *Rhinotridens britskii*, paratype, MZUSP 129867, 15.2 mm SL; dorsal view. ABb, additional basibranchial element; Bb2-4, basibranchials 2 to 4; Cb1-5, ceratobranchials 1 to 5; Eb1-4, epibranchials 1 to 4; Hb1-3, hypobranchials 1 to 3; Pb3-4, pharyngobranchials 3 to 4; Utp, upper pharyngeal tooth plate. Scale bar = 0.1 mm.

fully visible in both lateral and ventral views and positioned immediately anterior to pectoral-fin base, with 5 exposed conical odontodes. Opercular and interopercular odontodophores not juxtaposed, instead well separated by space equivalent minimally to diameter of former (Fig. 6). Branchiostegal membrane forming free fold ventrally across isthmus, its posterior margin gently sinusoid, broadly concave medially (Fig. 2). Cephalic latero-sensory system pores four on each side of head (Figs. 2B–C). Posterior one (L1, visible clearly in Fig. 2B, and faintly in profile in Fig. 2A) positioned dorsomesially to opercular odontodophore; second pore (prec, visible clearly in Fig. 2A) laterally-oriented, horizontally aligned with middle of opercular odontodophore and vertically aligned with middle of interopercular odontodophore; third one (infc, visible in Figs. 2A–B, right side) approximately midway between posterior margin of eye and base of opercular odontodophore, fourth and anterior-most pore (s3, visible in Fig. 2B, right side) closer to dorsal midline than all others, positioned approximately at transverse line through posterior third of eyes. Lateral-line short, reduced to short branch extending posteriorly from area of posterior margin of opercular odontodophore, with one laterally-oriented pore approximately at midlength of canal (Figs. 2–6), and posterior terminal pore, posteroventrally-bent, positioned at vertical through middle of pectoral fin (Fig. 2). Axillary gland large and tumescent in some specimens, surrounding pectoral-fin base on all sides except anteriorly, extending posteriorly to almost margin of pectoral fin (Fig. 1) and opening posteriorly as a large slit-like pore (not visible in illustrations). Gland small and inconspicuous in some other specimens.

Pectoral fin small, *ca*. 40–45% of HL, its rays similar in length, forming slightly convex distal margin (Fig. 1). Pectoral-fin rays i,4(18*), i,3(3) or ii,1,i(1), count asymmetrical in three specimens (one of which holotype, with i,4 on right side and i,5 on left side; first

TABLE 1 | Morphometric data for holotype and paratypes of *Rhinotridens britskii*; range includes holotype. N = number of specimens; SD = Standard deviation.

	Holotype	Range	Mean	SD	N
Standard length (mm)	15.2	13.4–16.5	–	–	12
Percentage of standard length					
Body depth	14.9	13.1–18.2	15.7	1.5	12
Caudal peduncle length	10.2	8.4–11	9.9	0.7	12
Caudal peduncle depth	8.0	7.4–8.9	8.3	0.4	12
Predorsal length	73.6	67.5–74.2	71.5	2.0	12
Preanal length	61.8	55.5–62.7	59.8	2.1	12
Dorsal-fin base length	8.4	6.9–10.2	8.9	1.0	12
Anal-fin base length	31.4	29–35.1	32.4	1.9	12
Distance between dorsal-fin origin and caudal-fin base	31.1	29.5–34.1	31.4	1.5	12
Distance between anal-fin origin and caudal-fin base	41.6	38.8–44.4	41.8	1.7	12
Pectoral girdle width	11.6	11.1–13.7	12.3	0.8	12
Pectoral fin length	7.9	7.1–10.4	8.8	0.8	12
Prepelvic length	47.4	42.7–47.4	45.2	1.3	12
Percentage of head length					
Head length	17.3	17.3–19.9	18.6	0.8	12
Head width	71.8	66.2–73.5	71.2	1.9	12
Head depth	56.5	43.2–56.5	50.4	3.4	12
Interorbital distance	32.9	31.2–39.4	34.9	1.9	12
Snout length	37.2	37.2–43.2	40.2	1.7	12
Maxillary-barbel length	-	8.3–20.1	8.0	3.6	7
Mouth width	51.6	37.7–51.6	45.0	3.8	12
Eye diameter	28.8	26.1–29.7	28.1	0.9	12

ray distally branched on one side of few specimens), first ray not prolonged as filament. Pelvic fin small (Fig. 1), located on anterior half of SL, distant from anal-fin base by distance equivalent to pelvic fin length or slightly more. Pelvic-fin rays i,4(20*) (Fig. 10), with last ray sometimes not branched or only incipiently branched. Pelvic splint absent (Fig. 10). Dorsal fin with distal margin gently convex, its origin slightly posterior to that of anal fin (Fig. 1). Dorsal-fin rays vii(2), viii(18*), or ix(1), with second to fourth rays incipiently branched in some specimens. Anal fin long (Fig. 1), with distal margin strait to slight concave, posteriorly adjacent to area of lower procurrent caudal-fin rays. Anal-fin rays xxii(1), xxiii(3), xxiv(4), xxv(4), xxvi(5*), xxviii(1) or xxix(2), plus one procurrent ray. Caudal fin shallowly emarginate, with upper lobe slightly longer than lower one. Caudal-fin rays 6/6(1), 6/7(18*), 6/8(1) or 7/8(1). Procurrent caudal-fin rays 7–10 dorsally and 7–12 ventrally.

Neurocranium. Skull roof mostly unossified, forming single large fontanel bordered by mesethmoid, frontal, sphenotic-prootic-pterosphenoid, and parieto-supraoccipital (Fig. 5). Mesethmoid formed by thin lamina of bone, T-shaped in dorsal view, with broad central shaft, connected to anterior, cornua-bearing portion by extremely thin

hinge-like sheet of bone bent 90° ventrally (visible only faintly in Fig. 5A). Distal part of cornua strongly bent ventrolaterally, its tip slightly bent posteriorly. Mesethmoid stem covered posterodorsally by anterior part of frontals. Frontal elongate, its posterior two-thirds rod-like, forming narrow rim at dorsolateral margin of neurocranium (Fig. 5). Its anterior third expanded and chisel-like, meeting its antimere sagittally. Sphenotic, prootic, and pterosphenoid fused. Portion corresponding to sphenotic very narrow

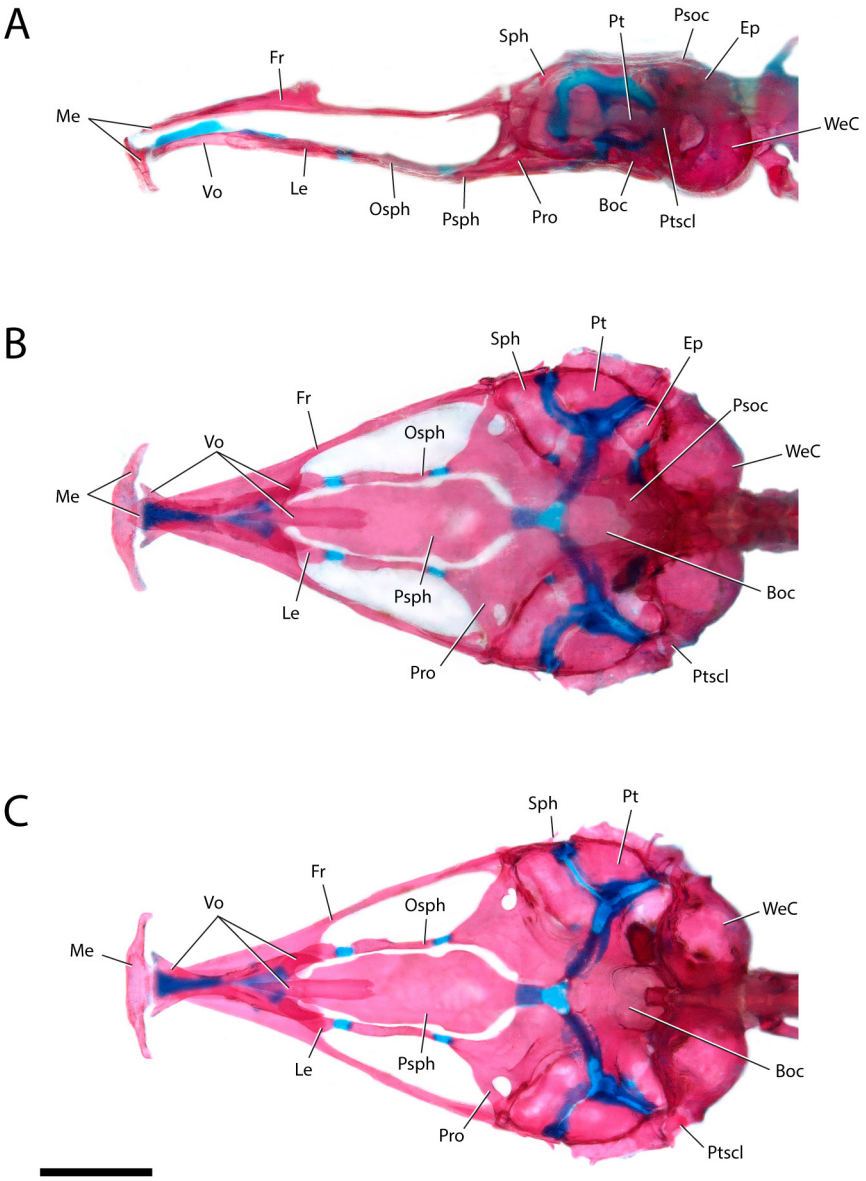

FIGURE 5 | Neurocranium and associated structures of *Rhinotridens britskii*, paratype, MZUSP 129867, 15.2 mm SL; **A.** Lateral view; **B.** Dorsal view; **C.** Ventral view. Boc, basioccipital; Ep, epioccipital; Fr, frontal; Le, lateral ethmoid; Me, mesethmoid; Osph, orbitosphenoid; Psph, parasphenoid; Psoc, parieto-supraoccipital; Ptscl, postemporo-supracleithrum; Pro, prootic; Pt, pterotic; Sph, sphenotic-prootic-pterosphenoid; Vo, vomer; WeC, Weberian capsule. Scale bar = 0.5 mm.

anteriorly, matching in shape (and connected to) posterior end of frontal. Parieto-supraoccipital with curved anterolateral projections bordering posterolateral portion of cranial fontanel. Pterotic with small lateral process. Vomer large, roughly hourglass-shaped, forming most prominent element at ventral aspect of ethmoid region. Anterior end of vomer flared and truncate, ending immediately posterior to base of mesethmoid cornua and with small anterolateral process on each side, contacting base of mesethmoid cornua (Fig. 5). Posterior part of vomer expanded and split into three large processes. Median process longest, with round distal end, overlapping ventrally central part of parasphenoid. Lateral arms shorter, pointed and claw-like, ventrally overlapping most of lateral ethmoid. Midlength of vomer with lateral thickening forming facet for articulation with autopalatine. Lateral ethmoids small and simplified, restricted to neurocranial floor, straight in ventral aspect, converging anteriorly towards midline and separated from each other by anterior part of parasphenoid (Figs. 5B, C). Lateral ethmoid connected by cartilage with anterior end of orbitosphenoid posteriorly and with ethmoid cartilage anteriorly (Fig. 5). Orbitosphenoid rod-like, straight, or gently sigmoid, lacking foramina, and restricted to neurocranial floor. Parasphenoid broad and laminar, suspended mostly on soft tissue of the skull floor, free from surrounding bones except anteriorly with vomer and posteriorly with prootic symphysis (Figs. 5B, C). Basioccipital lacking anterior processes and not sutured to parasphenoid. Latero-sensory canal enclosed by bone in supracleithrum and pterotic, extending anteriorly to that point in soft tissue only, alongside sphenotic and most of frontal, diverging laterally from skull margin anteriorly and ending at pore slightly posterior to anterior margin of eye.

FIGURE 6 | Scanning electron microscopy of the opercular region of *Rhinotridens britskii*, paratype, MZUSP 36303, 13.4 mm SL. Arrows indicate opercular odontodophore (dorsally) and interopercular odontodophore (ventrally). Scale bar = 0.1 mm.

Jaws. Premaxilla large, with general claw-like shape in dorsal view, with long recess along distal two-thirds of posterior margin tapering distally, and with conspicuous anteromedial ascending process articulating with posterior margin of mesethmoid cornua (Fig. 3). Premaxillary teeth disposed in three arched rows implanted on bone (with 29, 32, and 26 teeth each, anterior to posterior), plus three additional rows of labial teeth (with 5, 11–12, and 20 teeth each, anterior to posterior) attached to upper-lip connective tissue just anterior to premaxilla, in arrangement continuous with that of bone-attached dentition (Fig. 3). Posteromedial margin of premaxilla protruded, bearing conspicuously independent dentition, with 5–6 teeth disposed in semicircle (Fig. 3). Maxilla small, paralleling concave posterior profile of premaxilla and distally supporting internal cores of maxillary and rictal barbels, proximally with finger-like articular process hinged on anterior margin of distal portion of anterior autopalatine cartilage (Fig. 3). Lower jaw heavily ossified, much wider (transversely) than long (longitudinally). Articulation with quadrate modified into posteromedially-directed process attached nearly at middle of lower jaw, formed mostly by compound articular (= angulo-articulo-retroarticular). Coronoid process possible represented by small process distal to that articulation. Dentary with numerous teeth arranged in five well-defined rows (visible in straight view against toothed surface) disposed in curved files oblique to longest axis of lower jaw, with 4–6, 10–11, 16, 17–18, and 17–18 teeth). Teeth at symphysis more mesially-oriented than remainder of dentary dentition, apparently providing counterpart to offset premaxillary dentition dorsally. Meckel's cartilage small and located just ventral to the last row of dentary teeth. Coronomeckelian bone absent.

Suspensorium and opercular series. Autopalatine asymmetrically stellate in general aspect, with hypertrophied lateral process pointed and directed straight laterally, its anterior margin slightly posterior transversely to anterior margin of main body of bone (Fig. 3). Anterior autopalatine cartilage elongated laterally, originating on anterior surface of main body of bone and extending laterally alongside anterior margin of lateral process, closely positioned to latter but unattached to it. Mesial process of autopalatine thick and broad-based, forming articulation with neurocranium via vomer. Deep concave recess anteromesially between main body of autopalatine and mesial process, matching area of posteromesial offset tooth platform of premaxilla (see above). Posterior autopalatine process long and thin, with no distal cartilage, curved ventrally towards ascending process of quadrate but not contacting it, instead ligamentously connected with anterodorsal process of hyomandibula. Quadrate with anterior portion laminar and posterior portion elongate, its ascending process with large cartilage plug fitting into anterior recess on anterodorsal hyomandibular process (Fig. 7). Metapterygoid absent. Hyomandibula with large distal process directed anterodorsally, split into unequal-sized branches, larger one spike-like and pointed, smaller one truncated. Dorsal margin of hyomandibula with pointed protrusion approximately at its midlength (Fig. 7). Hyomandibula with triple link with skull: by small cartilage plug articulating at pterotic-sphenotic cartilage limit, by short ligament (originating on ventral surface of pterotic and inserted on posterodorsal hyomandibular process immediately posterior to cartilage articulation) and by direct bony link with ventral part of sphenotic. Preopercle with anterior half narrow, pointed and curved dorsally. Small ventral condyle present for articulation with interopercle. Interopercle short, with dorsal concavity for articulation with opercle and odontodophore bearing five similar-sized odontodes in

single row. Opercle with considerable laminar area, conspicuous adductor crest, and well-defined dilatator process positioned immediately dorsal to large articular facet with hyomandibula. Opercular odontodophore compact, with four clustered odontodes. Anteroventral process of opercle short, laminar, and broad in lateral view.

Hyoid bar. Urohyal with short and thin lateral arms not reaching branchiostegals, short posterior process, and hyoid foramen widely variable in size (Fig. 8). Ventral (and only) hypohyal with large ventral fovea for articulation with blunt urohyal condyles. Anterior ceratohyal straight, flattened at articular extremities, their planes oriented orthogonally relative to each other. Posterior ceratohyal short and conical. Interhyal absent. Branchiostegals six, increasing only slightly in length posteriorly. Three branchiostegals articulating with anterior ceratohyal, two with posterior ceratohyal and one with intervening cartilage.

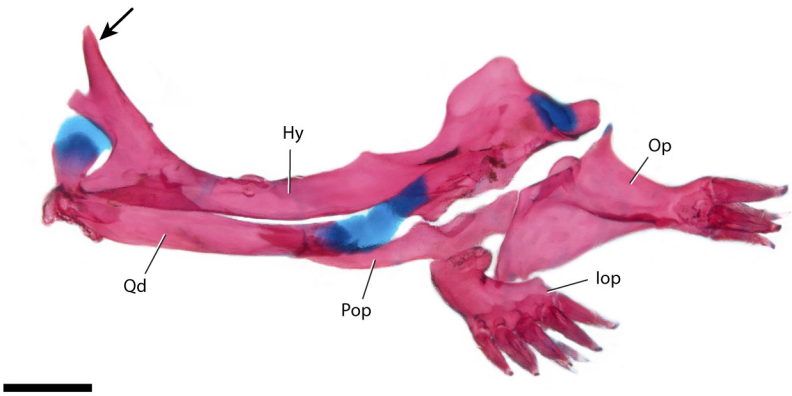

FIGURE 7 | Suspensorium and opercular series of *Rhinotridens britskii*, paratype, MZUSP 129867, 15.2 mm SL; left lateral view. Arrow indicates distal process of hyomandibula. Hy, hyomandibular; Iop, interopercle; Op, opercle; Pop, preopercle; Qd, quadrate. Scale bar = 0.2 mm.

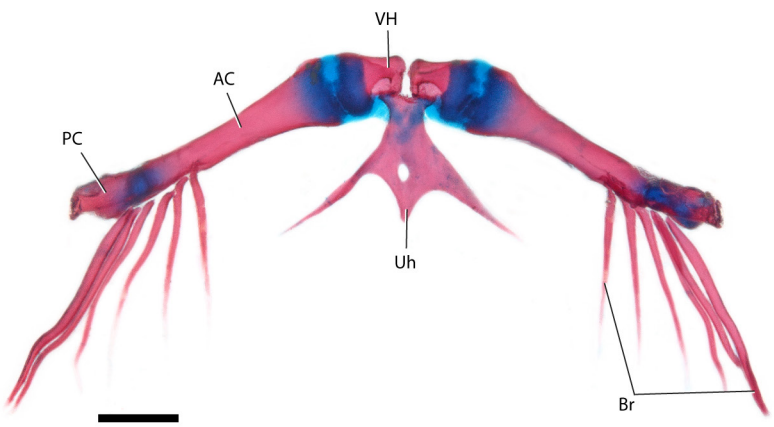

FIGURE 8 | Hyoid arch of *Rhinotridens britskii*, paratype, MZUSP 129867, 15.2 mm SL; ventral view. AC, anterior ceratohyal; Br, branchiostegal rays; PC, posterior ceratohyal; Uh, urohyal; VH, ventral hypohyal. Scale bar = 0.2 mm.

Gill arches. Basibranchials and hypobranchials completely cartilaginous (Fig. 4). Basibranchials 2 and 3 slender, conjoined in elongate anterior copula; basibranchial 4 short, nearly as broad as long, roughly hexagonal, sometimes preceded by spurious cartilage bodies resembling accessory basibranchial elements (such as specimen illustrated in Fig. 4). Hypobranchials 1 and 2 rod-like, their main axis oblique relative to longitudinal axis, more strongly so in latter. Hypobranchial 3 largest of series, complex-shaped and angulate, its main axis nearly parallel to longitudinal axis. Ceratobranchials ossified at middle portion, cartilaginous distally to tips. Ceratobranchials 1–4 with variably-shaped laminar projections; ceratobranchial 5 shorter and simpler in shape than rest of series, lacking teeth entirely (*i.e.*, lower pharyngeal dentition absent). Epibranchials 1–3 thinly ossified at middle portion, cartilaginous distally to tips. Epibranchial 1 with small anterodorsal uncinate process; epibranchials 2 and 3 slender, rod-like, latter articulating with anterior half of pharyngobranchial 3; epibranchial 4 wider and more densely ossified than others, articulating with posterior half of upper pharyngeal toothplate. Pharyngobranchial 4 cartilaginous, long, and rod-like, adpressed to large curved upper pharyngeal toothplate bearing four to six large teeth. Pharyngobranchial 3 represented by small independent cartilage immediately anterior to and aligned with pharyngobranchial 4 (Fig. 4). Gill rakers absent.

Axial skeleton and median-fins supports. Weberian apparatus encapsulated with narrow lateral opening with short neck-like extension (Fig. 5). Post-Weberian vertebrae 36(4), 37(3), or 39(1). First post-Weberian vertebra nearly half length of subsequent one. First complete haemal arch and spine on third post-Weberian vertebrae. Pleural ribs two, second pair smaller than first (vestigial in some specimens) and not contacting parapophyses. Dorsal-fin basal radials 8(6) or 9(2), first one posterior to hemal spine of post-Weberian vertebra 20(6) or 21(2). Anal-fin basal radials 27(4) or 29(2), first one posterior to hemal spine post-Weberian vertebra 15(3) or 16(5). Distal heads of first and second anal-fin radials expanded, at least twice as broad as those of subsequent elements. Hypural complex composed of two roughly triangular plates, lower one (supposed to represent fused parhypural and hypurals 1–2) larger in area than upper one (presumably formed by fused hypurals 3–5). Urostyle continuous with compound caudal centrum (PU1+U1), its basal half adpressed to dorsal margin of upper hypural plate and its distal half separated from latter by narrow gap. Epurals absent.

Paired girdles. Posttemporo-supracleithrum tightly articulated with neurocranium (Fig. 5). Cleithrum continuously ossified only at margins, with middle portion either totally unossified or ossified fragmentarily (Fig. 9). Posterior margin of cleithrum with well-defined articular surface for anteroventral surface of Weberian capsule. Scapulo-coracoid elongate and cylindrical, mineralized only at base in most specimens (in one specimen ossified entirely), distally supporting first proximal radial and first pectoral-fin ray (Fig. 9). First proximal radial reduced to a rod-like cartilaginous structure. Second proximal pectoral radial, distally flared (fan-shaped), mostly cartilaginous (with thin sheath of ossification, more heavily proximally) (Fig. 9). Basipterygia mostly cartilaginous, fused sagittally, with poorly mineralized ossification and two anterior arms broadly fused at base (Fig. 10). External arms directed straight anteriorly or anterolaterally, internal arms converging towards midline to meet at midline, in most

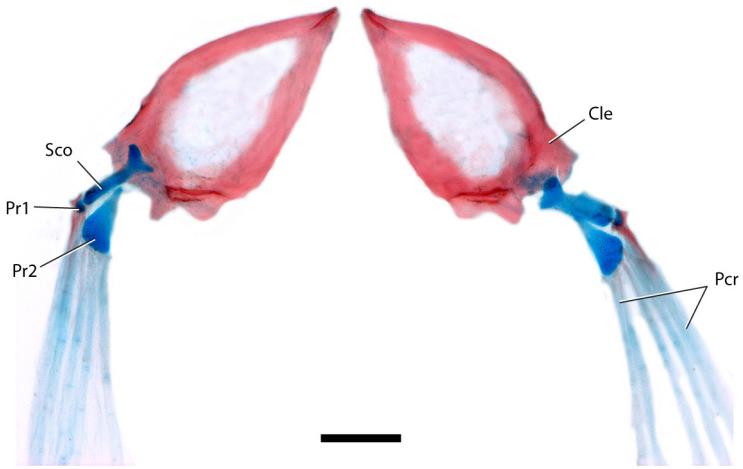

FIGURE 9 | Pectoral skeleton of *Rhinotridens britskii*, paratype, MZUSP 129867, 15.2 mm SL; ventral view. Cle, cleithrum; Pcr, pectoral-fin rays; Pr1-2, proximal radials 1-2; Sco, scapulocoracoid. Scale bar = 0.3 mm.

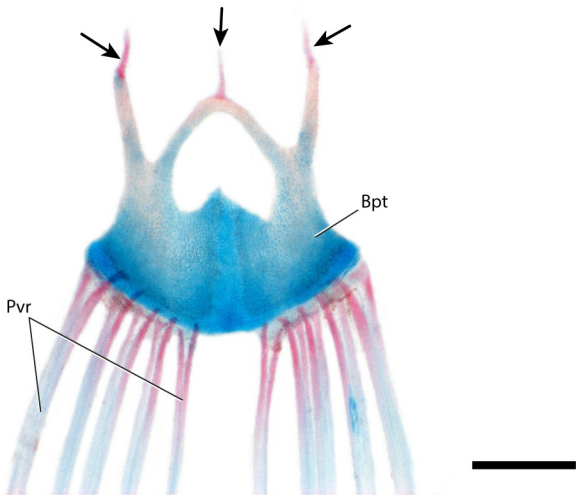

FIGURE 10 | Pelvic girdle and fin of *Rhinotridens britskii*, paratype, MZUSP 129867, 15.2 mm SL. Arrows indicate ossified tips of basipterygium arms. Bpt, basipterygium; Pvr, pelvic-fin rays. Scale bar = 0.2 mm.

specimens fusing into median process directed anteriorly. Various minor deformities/polymorphism in basipterygial morphology. Single specimen in ZUEC 15118 with more heavily mineralized basipterygia. Intervening cartilage remains continuous in that specimen. Pelvic splint absent.

Coloration in alcohol. Head with dense covering of dark chromatophores on dorsal and lateral surfaces of snout, extending posteriorly along margins of braincase (Fig. 1). Central portion of braincase (corresponding mostly to hypertrophied cranial fontanel) uniformly dark with dense brain pigment, medially delimiting striking white pupil chromatically simulating pseudo-fontanel (actual fontanel not corresponding to white

shape). Dark pigment of head extending ventrolaterally to cheeks and region around base of pectoral fin. Dark irregular concentrations on bases of odontodophores. Narrow dark markings regularly arranged between individual odontodes (most pronouncedly on interopercular odontodophore). Ventral surface of head mostly white, except for anterior portion of snout and occasional random spots in some specimens. Lips and maxillary barbels white. Entire dorsum densely covered with dark chromatophores, laterally disposed in poorly-defined file, extending onto dorsal margin of caudal peduncle as row of dark spots. Entire length of longitudinal skeletogenous septum outlined with thin row of dark chromatophores, all the way to base of hypural plate, forming conspicuous midlateral stripe. Thin broken lines of dark chromatophores faintly outlining limits of anterior epaxial myotomes. Well-defined row of spots forming mostly continuous dark line along entire base of anal fin, with small concavities between individual fin-ray bases. Dorsal to that, second dark line of spots along lower limit of hypaxial musculature, two lines posteriorly converging to end of anal-fin base. Individual fin-rays of all fins irregularly outlined with interspersed narrow dark fields, most intense on first pectoral-fin ray and least intense on pelvic fins. Bases of pelvic and pectoral fins with intense irregular dark fields. Base of dorsal fin with nearly continuous dark line. Ray-bearing margin of hypural plate intensely darkly outlined. Densely-set melanophores at dorsal region of peritoneum forming large abdominal dark region between pectoral region and anus, visible through thin abdominal wall. One specimen in MZUSP 72077 abnormally dark, due both to expanded dark chromatophores throughout body and head, and also to darker than usual background color (latter trait perhaps result of preservation history). Other than for its intensity, general coloration pattern of that specimen matching that of normal specimens.

Geographical distribution. *Rhinotridens britskii* is known from the lowland Amazon basin at rio Solimões, rio Purus, rio Madeira, and Ati-Paraná (a long river-like channel linking the rio Solimões with the rio Japurá), all in Amazonas State, Brazil, and in the river confluence at Río Amazonas called Río Loretoyacu in Colombia, and Río Yanayaco in Peru (Fig. 11).

Ecological notes. Data on the ecology of the specimens collected in the type-locality were kindly provided by two of the collectors, F. C. T. Lima and C. Moreira. The igarapé Boa Vista at the collection site (Fig. 12) has lightly-stained black water, diverging in that regard from a majority of other water courses in that region, which are mostly clear water. There had been heavy rains in the days preceding the collection, which flooded the igapó forest. Specimens of *R. britskii* were collected in the flooded forest, swimming in midwater. Specimens of *R. britskii* have been recorded from the same collection event as *Tridentopsis brevis* (Eigenmann & Eigenmann, 1889) on at least two occasions: on the type-locality of the former (MNRJ 53146) and at Ati-Paraná (a long river-like channel linking the rio Solimões with the rio Japurá) (MZUSP 36303). This indicates that the two species are sympatric. It is unknown whether or not they were also syntopic.

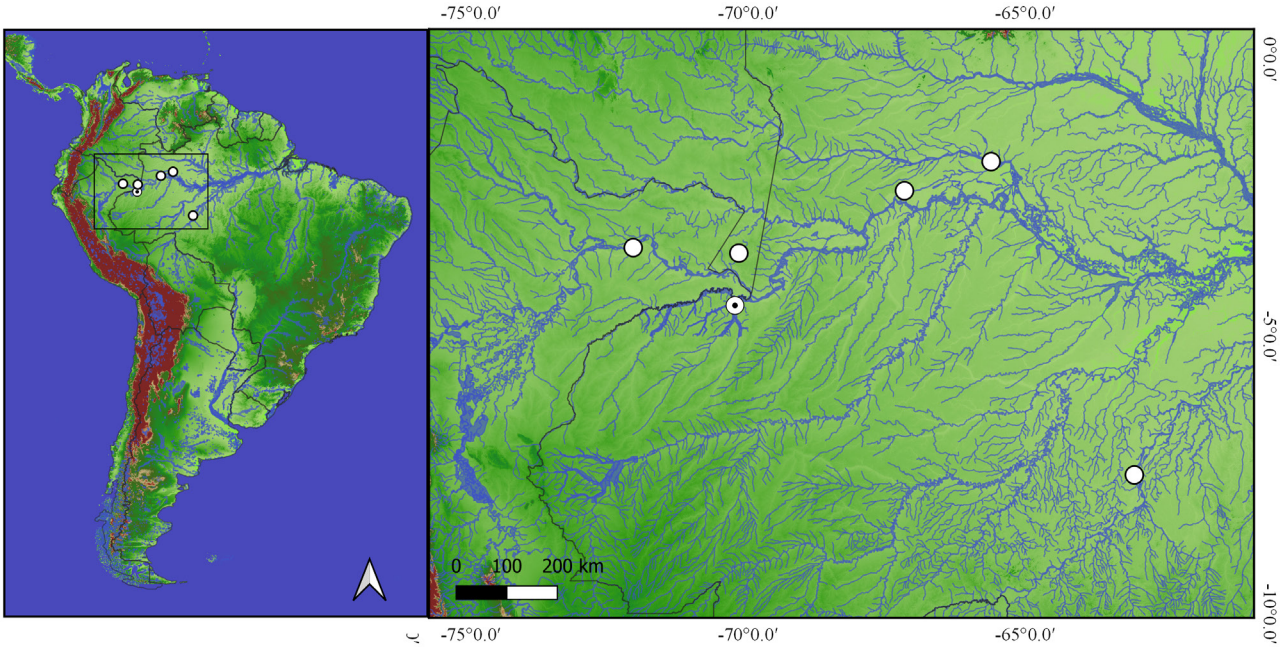

FIGURE 11 | Geographic distribution of *Rhinotridens britskii*. Dotted circle, holotype; white circle, paratypes and non-type specimens.

FIGURE 12 | Type-locality of *Rhinotridens britskii*, igarapé Boa Vista (rio Javari drainage), Atalaia do Norte Municipality. Photo by Flávio C. T. Lima.

Etymology. Named in honor of Heraldo Britski, first collector of specimens of the new species, in recognition of his pivotal role in the development of ichthyology in Brazil and also as a token of his 90th birthday in 2024. A noun in a genitive case.

Conservation status. *Rhinotridens britskii* is spread over a large geographic range, including localities in Brazil (rio Purus, rio Madeira, and Ati-Paraná), in Colombia (Río Loreto-Yacco) and in Peru (Río Yanayacu). No significant threats to the species have been identified in its area of occurrence. Thus, we believe *R. britskii* can be provisionally classified as Least Concern (LC) according to the categories and criteria of the International Union for Conservation of Nature (IUCN Standards and Petitions Committee, 2022).

Remarks. Specimens MCZ 52186, MZUSP 72977 and MZUSP 121256, respectively from Colombia, Brazil (rio Madeira) and Peru, conform to all external characteristics of *R. britskii* as in the Diagnosis and generally also fit within or adjacent to the morphometric ranges of other specimens from the type-locality and surroundings, although often in one end of the spectrum. The only significant difference found was in caudal peduncle depth of MCZ 52186 and MZUSP 121256 (6.5–6.8 and 6.9% SL, respectively), less deep than that of types (7.4–8.9% SL) (Tab. 2). This difference alone is not enough for inferring taxonomic differentiation, although it may indicate some form of geographical variation, pending additional study and material from respective localities. For these reasons, the specimens are not designated as paratypes.

TABLE 2 | Morphometric data for five non-type specimens of *Rhinotridens britskii* (MZUSP 72977; MZUSP 121256; MCZ 52186). N = number of specimens.

	MZUSP 72977	MZUSP 121256	MCZ 52186 (N = 3)
Standard length (mm)	14.8	15.2	14.1–15.3
Percentage of standard length			
Body depth	14.8	12.7	12.8–13.8
Caudal peduncle length	11.9	9.6	7.9–11.9
Caudal peduncle depth	7.7	6.9	6.5–6.8
Predorsal length	69.6	67.3	70.2–72.1
Preanal length	59.0	56.8	59.5–61.4
Dorsal-fin base length	8.9	7.9	8.0–10.7
Anal-fin base length	30.7	32.9	29.6–32.6
Distance between dorsal-fin origin and caudal-fin base	33.0	30.8	30.2–31.6
Distance between anal-fin origin and caudal-fin base	43.0	42.1	39.5–40.8
Pectoral girdle width	12.4	9.7	11.1–11.8
Pectoral fin length	8.5	7.5	8.2–8.7
Prepelvic length	41.7	42.4	45.2–45.9
Percentage of head length			
Head length	19.0	18.7	18.9–19.5
Head width	70.1	62.6	63.8–65.7
Head depth	49.0	39.9	42.4–45.6
Interorbital distance	28.9	29.4	29.3–31.4
Snout length	38.3	40.2	41.7–42.7
Maxillary-barbel length	–	–	8.7–10.8
Mouth width	45.4	42.5	34.5–37.3
Eye diameter	24.6	30.2	24.5–26

DISCUSSION

There is little doubt that *Rhinotridens britskii* is the sister group of *R. chromocaudatus* and thus that the genus is monophyletic as composed of the two species. The synapomorphies proposed for *Rhinotridens* in Datovo *et al.* (2023) are: opercular and interopercular odontodophores separated by a large interspace (Figs. 6, 7; reversal of the condition at the base of the Tridentinae); snout with a conspicuous anteromedial protuberance (Figs. 1, 2); mesethmoid cornua directed ventrolaterally (Fig. 5); postero-symphyseal cluster of premaxillary teeth offset from remainder of premaxillary dentition, with teeth directed posteromedially (Fig. 3); distal process of hyomandibula directed anterodorsally (Fig. 7); rod-like orbitosphenoid ossified only ventral to the optic nerve (Fig. 5); and basipterygia fused sagittally (Fig. 10). All preceding characters are present in *R. britskii* in conditions very similar to those in *R. chromocaudatus* and do not require further explanation beyond those provided by Datovo *et al.* (2023). An additional synapomorphy from the morphology of the autopalatine may be added to that list. Uniquely in the two species of *Rhinotridens*, the lateral process of the autopalatine is hypertrophied, forming a prominent spike-like structure directed straight laterally (approximately as long as the width of the body of the autopalatine in *R. chromocaudatus* and proportionally even longer than that in *R. britskii*; compare Fig. 3 with fig. 3 in Datovo *et al*., 2023). This spike-like process of *Rhinotridens* spp. is not the cartilage-bearing arm, which is particularly prominent in species of *Tridens* and *Tridentopsis*, but rather a hypertrophied secondary process adjacent to that arm, immediately posterior to the base of its associated cartilage. The shape, position in the bone, and relationship to surrounding structures all support that the process is homologous in the two species of *Rhinotridens*. In all other tridentines the lateral autopalatine process, when present, is far shorter than the width of the autopalatine body or even vestigial.

In dorsal view, the offset, posterosymphyseal premaxillary teeth (and their apparent dentary counterparts) in both *R. britskii* and *R. chromocaudatus* are aligned with the deep semicircular concavity in the anteromesial margin of the autopalatine (seen posterior to the posterosymphyseal tooth patch in Fig. 3). Moving mouth parts in c&s specimens shows that the offset premaxillary dentition fits into that anterior autopalatine recess in part of the range of movement. It seems probable that such linkage is biomechanically related to movements of the mouth apparatus during feeding. The unusual nature of such configuration suggests some specialized feeding mechanics probably linked to equally specific feeding habits.

A few qualitative characters clearly distinguish *R. britskii* from its only congener *R. chromocaudatus*, as summarized in the Diagnosis above. Of those, the lack of a dark horizontal stripe along the middle of the caudal fin (Fig. 1) is plesiomorphic, since a monochromatic caudal fin is the condition in all other tridentines. Of remaining diagnostic characters, the straight shape of the orbitosphenoid in *R. britskii* (Fig. 5) is also plesiomorphic, as judging from the homologous portion of the bone also being mostly straight in other tridentines. The 22–29 segmented anal-fin rays and the interorbital larger than eye diameter are variable conditions in Tridentinae and their phylogenetic significance requires more detailed knowledge than is currently available about the ranges of those variables mapped onto a phylogeny of the subfamily. The absence of lower pharyngeal dentition (Fig. 4) is paralleled in other tridentine taxa, such

as in species of *Tridens*, and its phylogenetic significance is not decisive. That leaves the anteriorly-displaced position of the lateral spike-like process of the autopalatine (Fig. 3) as the only putative autapomorphy for *R. britskii*.

Rhinotridens britskii is a miniaturized trichomycterid, as all other Tridentinae. Miniaturization (*sensu* Weitzman, Vari, 1988) is an evolutionary phenomenon particularly prevalent in Trichomycteridae, wherein it happened once in the SGTSV-clade, with a few important reversals to larger sizes in Stegophilinae and Vandelliinae (DoNascimiento, 2013; Reis, 2022). Miniaturization often results in reductive paedomorphic features. For example, the absence of the lower pharyngeal dentition in *R. britskii* is an extreme condition of a general reduction of branchial arch elements in the SGTSV-clade (Reis, 2022).

Comparative material examined. Same listed in Datovo *et al*. (2023), plus *Tridentopsis brevis*: MNRJ 53146 (8 eth), MZUSP 36303 (12 eth, 2 c&s).

ACKNOWLEDGEMENTS

We are grateful to Flávio C. T. Lima (ZUEC) and Cristiano R. Moreira (MNRJ) for sharing first-hand field information about the collection of *Rhinotridens britskii*, as well as a photo of the habitat. Thanks to David Catania (CAS), Mary-A. Rogers and Caleb McMahan (FMNH), Michael Retzer (INHS), Roberto Reis, Carlos Lucena, and Zilda M. Lucena (MCP), Karsten Hartel (MCZ), Darío Mandelburger and Héctor S. Vera-Alcaraz (MNHNP), Cristiano Moreira, Carter Gilbert (UF), Carole Baldwin, G. David Johnson, Lynne Parenti, Richard Vari, Jeffrey Clayton, Kris Murphy, Diane Pitassy, and Sandra Raredon (USNM), and Flávio C. T. Lima, for kindly allowing the study of specimens under their care. We are also grateful to Lara Guimarães for help with SEM examination and to Dione Seripierri for untangling geographic localities. This study was supported by the Fundação de Amparo à Pesquisa do Estado de São Paulo (FAPESP #2023/02499–4 to AD; FAPESP #16/19075–9 to MNLP), Conselho Nacional de Desenvolvimento Científico e Tecnológico (CNPq #301082/95–2, #405643/2018–7, and #310688/2019–1 to MP), and Coordenação de Aperfeiçoamento de Pessoal de Nível Superior (CAPES, PhD fellowship and PROAP-MZUSP to VR).

REFERENCES

- **Arratia G, Huaquin L.** Morphology of the lateral line system and of the skin of diplomystid and certain primitive loricarioid catfishes and systematic and ecological considerations. Bonner Zool Mon. 1995; 36:1–110.
- **Baskin JN.** Structure and relationships of the Trichomycteridae. City University of New York. 1973.
- **Datovo A, Bockmann FA.** Dorsolateral head muscles of the catfish families Nematogenyidae and Trichomycteridae (Siluriformes: Loricarioidei): comparative anatomy and phylogenetic analysis. Neotrop Ichthyol. 2010; 8(2):193–246. https://doi.org/10.1590/S1679-62252010000200001

- **Datovo A, Ochoa L, Vita L, Presti P, Ohara WM, de Pinna MCC.** A new genus and species of miniature tridentine catfish from the Amazon basin (Siluriformes: Trichomycteridae). Neotrop Ichthyol. 2023; 21(3):e230076. https://doi.org/10.1590/1982-0224-2023-0076
- **DoNascimiento C.** Morphological evidence for the monophyly of the subfamily of parasitic catfishes Stegophilinae (Siluriformes, Trichomycteridae) and phylogenetic diagnoses of its genera. Copeia. 2015; 103(4):933–60. https://doi.org/10.1643/CI-14-132
- **DoNascimiento CL.** Sistemática y relaciones filogenéticas de la subfamilia de bagres parásitos Stegophilinae (Siluriformes, Trichomycteridae). [PhD Thesis]. Caracas: Universidad Central de Venezuela; 2013.
- **Eigenmann CH.** The Pygidiidae, a family of South American catfishes. Mem Carnegie Mus. 1918; 7:259–398.
- **Fricke R, Eschmeyer WN.** Eschmeyer's catalog of fishes: guide to fish collections. [Internet]. San Francisco: California Academy of Science; 2023. Available from: http://researcharchive.calacademy.org/research/ichthyology/catalog/collections.asp
- **Henschel E, Mattos JLO, Katz AM, Costa WJEM.** Position of enigmatic miniature trichomycterid catfishes inferred from molecular data (Siluriformes). Zool Scr. 2017; 47(1):44–53. https://doi.org/10.1111/zsc.12260
- **International Union for Conservation of Nature (IUCN). Standards and petitions committee.** Guidelines for using the IUCN Red List categories and criteria. Version 15.1 [Internet]. Gland; 2022. Available from: http://www.iucnredlist.org/documents/RedListGuidelines.pdf
- **Lundberg JG, Baskin JN.** The caudal skeleton of the catfishes, order Siluriformes. Am Mus Novit. 1969; 2398:1–49.
- **Ochoa LE, Datovo A, DoNascimiento C, Roxo FF, Sabaj MH, Chang J, Melo BF, Silva GSC, Foresti F, Alfaro M, Oliveira C.** Phylogenomic analysis of trichomycterid catfishes (Teleostei: Siluriformes) inferred from ultraconserved elements. Sci Rep. 2020; 10:2697. https://doi.org/10.1038/s41598-020-59519-w
- **Ochoa LE, Roxo FF, DoNascimiento C, Sabaj MH, Datovo A, Alfaro M, Oliveira C.** Multilocus analysis of the catfish family Trichomycteridae (Teleostei: Ostariophysi: Siluriformes) supporting a monophyletic Trichomycterinae. Mol Phyl Evol. 2017; 115:71–81. https://doi.org/10.1016/j.ympev.2017.07.007
- **Ørvig T.** A survey of odontodes ('dermal teeth') from a developmental, structural, functional and phyletic point of view. In: Andrews SM, Miles RS, Walker AD, editors. Problems in Vertebrate evolution. Linnean Society Symposium Series No. 4. 1977; p.53–75.
- **de Pinna MCC.** A new sarcoglanidine catfish, phylogeny of its subfamily, and an appraisal of the phyletic status of the Trichomycterinae (Teleostei, Trichomycteridae). Am Mus Novit. 1989; 2950:1–39.
- **de Pinna MCC.** Phylogenetic relationships of Neotropical Siluriformes (Teleostei: Ostariophysi): historical overview and synthesis of hypotheses. In: Malabarba LR, Reis RE, Vari RP, Lucena ZMS, Lucena CAS, editors. Phylogeny and classification of Neotropical fishes. Porto Alegre: Edipucrs; 1998. p.279–330.
- **de Pinna MCC.** The dawn of phylogenetic research on Neotropical fishes: a commentary and introduction to Baskin (1973), with an overview of past progress on trichomycterid phylogenetics. Neotrop Ichthyol. 2016; 14(2):e150127. https://doi.org/10.1590/1982-0224-20150127
- **de Pinna MCC, Dagosta FC.** A taxonomic review of the vampire catfish genus *Paracanthopoma* Giltay, 1935 (Siluriformes, Trichomycteridae), with descriptions of nine new species and a revised diagnosis of the genus. Pap Avulsos Zool. 2022; 62:e202262072. https://doi.org/10.11606/1807-0205/2022.62.072
- **de Pinna MCC, Kirovsky AL.** A new species of sand-dwelling catfish, with a phylogenetic diagnosis of *Pygidianops* Myers (Siluriformes, Trichomycteridae, Glanapteryginae). Neotrop Ichthyol. 2011; 9(3):493–504. https://doi.org/10.1590/S1679-62252011000300004
- **de Pinna MCC, Zuanon J.** The genus *Typhlobelus*: monophyly and taxonomy, with description of a new species with a unique pseudotympanic structure (Teleostei: Trichomycteridae). Copeia. 2013(3):441–53. http://dx.doi.org/10.1643/CI-13-007

- **Reis VJC.** Ontogeny and phylogeny in Trichomycteridae (Teleostei, Siluriformes): patterns in the development of morphological complexes. [PhD thesis]. São Paulo: Universidade de São Paulo; 2022.
- **Reis VJC, Lecointre G, de Pinna MCC.** The Trichomycteridae: an overview of the systematics and classification of the family. In: Arratia G, Reis R, editors. Catfishes. Forthcoming 2024.
- **Taylor WR, Van Dyke GC.** Revised procedures for staining and clearing small fishes and other vertebrates for bone and cartilage study. Cybium. 1985; 9(2):107–19.
- **Walker MB, Kimmel CB.** A two-color acid-free cartilage and bone stain for zebrafish larvae. Biotech Histochem. 2007; 82(1):23–28. https://doi.org/10.1080/10520290701333558
- **Weitzman SH, Vari RP.** Miniaturization in South American freshwater fishes; an overview and discussion. Proc Biol Soc Wash. 1988; 101(2):444–65.
- **Wosiacki WB.** Estudo das relações filogenéticas de Trichomycterinae (Teleostei, Siluriformes, Trichomycteridae) com uma proposta de classificação. [PhD Thesis]. São Paulo: Universidade de São Paulo; 2002.

AUTHORS' CONTRIBUTION

Mário de Pinna: Conceptualization, Data curation, Formal analysis, Investigation, Methodology, Project administration, Writing-original draft, Writing-review and editing.

Vinícius Reis: Data curation, Investigation, Methodology, Visualization.

Murilo N. L. Pastana: Data curation, Formal analysis, Visualization, Writing-review and editing.

Aléssio Datovo: Conceptualization, Data curation, Investigation, Methodology, Writing-review and editing.

ETHICAL STATEMENT

Not applicable.

COMPETING INTERESTS

The author declares no competing interests.

HOW TO CITE THIS ARTICLE

- **de Pinna M, Reis V, Pastana MNL, Datovo A.** A new species of the tridentine *Rhinotridens* from the Amazon basin (Siluriformes: Trichomycteridae). Neotrop Ichthyol. 2024; 22(2):e240025. https://doi.org/10.1590/1982-0224-2024-0025

Neotropical Ichthyology

OPEN ACCESS

Official Journal of the
Sociedade Brasileira de Ictiologia
SBI